ORIGINAL ARTICLE

JBMR

Bone Material Quality in Transiliac Bone Biopsies of Postmenopausal Osteoporotic Women After 3 Years of Strontium Ranelate Treatment

Paul Roschger,[1] Inderchand Manjubala,[2] Norbert Zoeger,[3,5] Florian Meirer,[3] Rolf Simon,[4] Chenghao Li,[2] Nadja Fratzl-Zelman,[1] Barbara M Misof,[1] Eleftherios P Paschalis,[1] Christina Streli,[3] Peter Fratzl,[2] and Klaus Klaushofer[1]

[1]Ludwig Boltzmann Institute of Osteology at the Hanusch Hospital of WGKK and AUVA Trauma Centre Meidling, 4th Medical Department, Hanusch Hospital, 1140 Vienna, Austria
[2]Max Planck Institute of Colloids and Interfaces, Department of Biomaterials, 14424 Potsdam, Germany
[3]Vienna University of Technology, Atominstitut, 1020 Vienna, Austria
[4]FLUO Beamline ANKA, Karlsruhe, Germany
[5]Nuclear Engineering Seibersdorf, 2444 Seibersdorf, Austria

ABSTRACT

Strontium ranelate (SrR) is a relatively new treatment for osteoporosis. In this study we investigated its potential impact on human bone material quality in transiliac bone biopsies from postmenopausal osteoporotic women treated 3 years with calcium and vitamin D plus either 2 g SrR per day or placebo. Bone mineralization density distribution (BMDD), strontium (Sr) concentration, collagen cross-link ratio, and indentation modulus were analyzed by quantitative backscattered electron imaging, electron-induced X-ray fluorescence analysis, synchrotron radiation induced micro X-ray fluorescence elemental mapping, Fourier transform infrared imaging, and nanoindentation, respectively. The BMDD of SrR-treated patients was shifted to higher atomic numbers (Z_{mean} +1.5%, $p < .05$ versus placebo). We observed Sr being preferentially incorporated in bone packets formed during SrR treatment up to 6% atom fraction [Sr/(Sr + Ca)] depending on the SrR serum levels of the individuals (correlation $r = 0.84$, $p = .018$). Collagen cross-link ratio was preserved in SR-treated bone. The indentation modulus was significantly decreased in younger versus older bone packets for both placebo- (−20.5%, $p < .0001$) and SrR-treated individuals (−24.3%, $p < .001$), whereas no differences were found between the treatment groups. In conclusion, our findings indicate that after SrR treatment, Sr is heterogeneously distributed in bone and preferentially present in bone packets formed during treatment. The effect of SrR on BMDD seems to be due mainly to the uptake of Sr and not to changes in bone calcium content. Taken together, these data provide evidence that the investigated bone quality determinants at tissue level were preserved in postmenopausal osteoporotic women after 3-year treatment with 2 g SrR per day plus calcium and vitamin D. © 2010 American Society for Bone and Mineral Research.

KEY WORDS: STRONTIUM RANELATE; OSTEOPOROSIS; BONE MATERIAL QUALITY; QBEI; SR-μXRF; FTIRI; NANOINDENTATION

Introduction

Strontium ranelate (SrR) is an innovative treatment of osteoporosis based on the Spinal Osteoporosis Therapeutic Intervention (SOTI)[1] and the Treatment of Peripheral Osteoporosis (TROPOS)[2] studies. A fracture risk reduction for postmenopausal osteoporosis after 3 years of treatment with 2 g/day SrR orally of 41% ($p < .001$) and 16% ($p = .04$), respectively, has been reported for vertebral and nonvertebral fractures.[1,2] Recently, efficacy on fracture risk reduction also was proven for 5 years of SrR treatment,[3] as well as treatment in osteopenic patients.[4] There is an intense research activity to elucidate the underlying mechanism of SrR antifracture efficacy, including bone microarchitecture, bone remodeling balance, and Sr interaction with the calcium-sensing receptors of bone cells.[5–10] In vertebrates, 99% of whole-body Ca and Sr is located in bone.[11] Thus every increase in serum level of Sr is likely to lead to a higher fraction of Sr in the bone tissue, as numerous studies, especially in animal models, have shown.[12–15] Interestingly, in these treatment studies, Sr seems to be hetero-

Received in original form May 13, 2009; revised form September 9, 2009; accepted October 15, 2009. Published online October 17, 2009.
Address correspondence to: Paul Roschger, PhD, Ludwig Boltzmann Institute of Osteolgy, UKH-Meidling, Kundratstr. 37, A-1120 Vienna, Austria.
E-mail: paul.roschger@osteologie.at

Journal of Bone and Mineral Research, Vol. 25, No. 4, April 2010, pp 891–900
DOI: 10.1359/jbmr.091028

geneously distributed within the whole skeleton (with higher Sr content at the iliac crest than at the femur and lumbar vertebra)[16] and even within the bone tissue of a single skeletal site, where individual bone packets exhibit different Sr contents.[15–17] The aim of this study was to elucidate the amount of the local Sr uptake and its influence on the bone material quality at the bone packet level in patients treated with SrR for 3 years. Important questions addressed in this context were (1) Does the amount of Sr incorporation depend on whether the bone packet is formed during SrR treatment or existed before treatment? (2) Does the amount of Sr incorporation depend on the age of the individual bone packet? and (3) Are there changes in intrinsic mechanical properties of the bone nanocomposite material that could be caused by changes in collagen cross-link pattern? For this purpose, transiliac biopsies of postmenopausal osteoporotic women treated with SrR or placebo were analyzed by nondestructive spatially resolved scanning techniques, including quantitative backscattered electron imaging (qBEI), electron-induced X-ray fluorescence energy dispersive X-ray analysis (ERF-EDX), synchrotron micro-X-ray fluorescence (SR-μXRF) elemental mapping, Fourier transform infrared imaging (FTIRI), and nanoindentation.

Methods and Materials

Bone biopsy samples

Transiliac bone biopsies from postmenopausal osteoporotic women that participated in the Spinal Osteoporosis Therapeutic Intervention (SOTI)[1] and the Treatment of Peripheral Osteoporosis (TROPOS)[2] studies were kindly provided by Company Servier (IRIS, Courbevoie CEDEX, France). Throughout the study, subjects received daily calcium abd vitamin D supplements depending on the baseline serum concentration of 25-hydroxyvitamin D. After a run-in period of 2 to 24 weeks of calcium and vitamin D depending on the severity of the deficiency of calcium/vitamin D, the subjects received 2 g/d SrR or placebo.[1] A total of 18 polymethylmethacrylate (PMMA)–embedded undecalcified bone biopsy samples were examined. Seven biopsies were from patients who had received 3 years of placebo (plus calcium/vitamin D), and seven biopsies were from patients who had received 3 years of 2 g/day SrR (plus calcium/vitamin D). Additionally, four biopsies from patients at baseline before treatment (one from the placebo group and three from SrR group) were analyzed. Together with a subset of the 3-year treatment groups, they formed a set of four paired biopsies (before and after treatment).

Quantitative backscattered electron imaging (qBEI)

qBEI was employed to visualize and quantify the local average atomic number of the target material (undecalcified bone tissue of 18 iliac biopsies). The physical principle of the technique is based on a quantification of the intensity of electrons backscattered from the surface of a sectioned bone area. The signal obtained is proportional to the weight fraction of calcium (Ca wt%) present locally in the embedded bone tissue in cases where the atomic number of the inorganic phase is formed predominantly by Ca ($Z = 20$) and P ($Z = 15$) in the form of carbonated hydroxyapatite embedded in the organic matrix ($Z \cong 6$). Full details of the technique have been described elsewhere.[18–20] However, in this study, a contribution of incorporated Sr atoms ($Z = 38$) in the bone matrix of SrR-treated patients could be expected; therefore, in these cases, a direct transformation of qBEI gray levels to calcium/mineral content was not possible or only an apparent Ca content could be given. Thus the material contrast (qBEI gray levels) was expressed in average Z numbers. Blocks containing PMMA-embedded undecalcified iliac bone samples were prepared for qBEI by grinding and polishing in order to obtain plane and parallel surfaces. The sample surface then was carbon coated. qBEI was performed in a digital scanning electron microscope (DSM 962, Zeiss, Oberkochen, Germany) equipped with a four-quadrant semiconductor backscattered electron detector. The microscope was operated at 20 keV electron energy and a probe current of 110 pA. The entire cancellous bone area was imaged by qBEI using a pixel resolution of 4 μm. From the gray-level images, gray-level frequency histograms were derived and converted by calibration[19] to bone mineralization density distributions (BMDDs). BMDD curves (see Fig. 1) indicate the frequency of pixels (y axis) corresponding to a given average atomic number Z (x axis) occurring throughout the cancellous bone area. For statistical analysis, four parameters characterizing these atomic number BMDD curves were determined (analogous to the BMDD curves with the gray levels expressed in Ca wt%) as described in detail elsewhere[19–21] (see Fig. 1):

- Z_{mean}, the weighted mean atomic number of the bone area obtained by the integrated area under the BMDD curve
- Z_{peak}, the peak position of the histogram, which indicates the most frequently occurring atomic number (value with the highest number of pixels) in the bone area
- Z_{width}, the full width at half maximum of the distribution, describing the variations in the atomic number values within the mineralized bone matrix

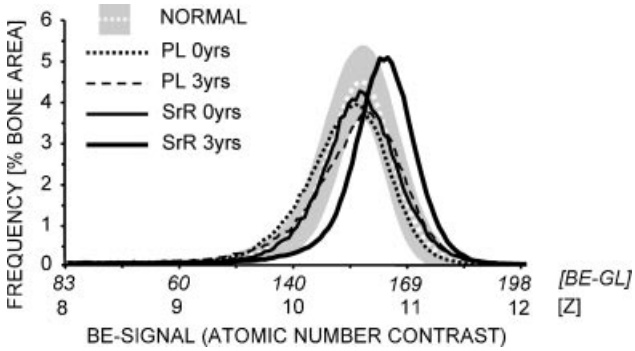

Fig. 1. Gray-level histograms (BMDD) from two paired bone biopsies as measured by qBEI. Pair one (*dashed lines*): PL0yrs and PL3yrs = BMDDs at baseline and after 3 years of placebo (Ca and vitamin D) treatment, respectively. Pair two (*solid lines*): SrR0yrs and SrR3yrs = BMDDs at baseline and after 3 years of strontium ranelate with Ca and vitamin D treatment, respectively. NORMAL = reference BMDD of normal adult trabecular bone.[20] X-axis: qBEI signal intensity in gray levels (BE–GL]) and in average atomic numbers of local bone material (Z); y axis: Frequency of appearance of a pixel bone area with a certain gray level or Z expressed in percent mineralized bone area.

- Z_{low}, the percentage of bone area that exhibits an atomic number below the fifth percentile of the reference BMDD of normal adults,[21] that is, below 9.58 (In the reference BMDD, this parameter corresponds to the amount of bone area undergoing primary mineralization.)

Analogous to these terms, Ca_{mean}, Ca_{peak}, Ca_{width}, and Ca_{low} (below 17.68 wt% percent calcium) were used when the BMDD was expressed in Ca content of the bone material in non-SrR-treated patients. It has to be emphasized that the relative changes in BMDD expressed in units of atomic numbers Z such as for Z_{mean}, Z_{peak}, and Z_{width} are always much smaller numerically than the corresponding values in BMDD expressed in units of Ca wt%. The reason for these differences is based on the different zero points of the two scales. In the case of Z values, zero means no material at all, whereas in the case of Ca wt%, zero means nonmineralized bone tissue (osteoid). To make the relative Z changes comparable with corresponding changes in Ca wt% units, the Z value of osteoid, which is approximately 6, has to be subtracted from the Z value first before calculation of the relative difference according the formula given below. Thus the adjusted relative differences in Z (adΔZ) are

$$\mathrm{ad}\Delta Z = 100 \times (Z_{after} - Z_{before})/(Z_{before} - 6)$$

In the following, an example for the difference between ΔZ and adΔZ using the Z_{mean} parameter values of the BMDDs from Fig. 1 (before $Z_{before} = 10.508$ and after $Z_{after} = 10.731$SrR treatment) is given:

$$\begin{aligned}\Delta Z &= 100 \times (Z_{after} - Z_{before})/(Z_{before}) \\ &= 100 \times (10.731 - 10.508)/10.508 = 2.1\%\end{aligned}$$

$$\begin{aligned}\mathrm{ad}\Delta Z &= 100 \times (Z_{after} - Z_{before})/(Z_{before} - 6) \\ &= 100 \times (10.731 - 10.508)/(10.508 - 6) \\ &= 4.9\%\end{aligned}$$

Electron-induced X-ray fluorescence energy dispersive X-ray analysis (EFR-EDX)

The local amount of the element Sr in the bone material was determined using the aforementioned scanning electron microscope (SEM) equipped with a LINK eXL system with a Pentafet germanium detector (Oxford Instruments, High Wycombe, England). The backscattered electron imaging mode was employed to select single bone packets for small-area scanning ($10 \times 10\,\mu m^2$) to acquire an X-ray fluorescence spectrum. On average, 30 bone packets per biopsy with about an equal number of lower and higher BEI gray levels were analyzed. For this purpose, the SEM was operated at 20 keV beam energy and a probe current of 0.220 nA (twice the beam current used for qBEI analysis to have sufficient counting statistics for spectral analysis with the beam damage effect to the bone tissue negligible). Data acquisition time was set to 500 seconds for each small-area scan. Quantification of the bone material elements was done by spectral peak analysis. Since the analysis was performed on a thick sample and not a thin-film sample, the interactions of the emitted X-rays with the surrounding matrix elements in the depth of the samples had to be taken into account. This was done by the ZAF method (software provided by Oxford Instrument), correcting for the atomic number and the absorption and fluorescence effects. EDX profiles of reference standards with known composition (wt% of the elements) were employed for quantification of the elements K, Na, Mg, Cl, S, P, Ca, and Sr. For example, for Ca and P the mineral apatite was used, and for S and Sr, celestine ($SrSO_4$, MAC, Micro-Analysis Consultants, Ltd., St. Eves, UK) was used. Since the light elements such as H, O, C, and N could not be measured directly (limitations of the detector), their contribution, basically reflecting the organic matrix, was determined as complement to 100% of all the other elemental wt% contributions. For the ZAF correction of the organic matrix, C was used as a representative element. EDX was done on all 18 bone biopsies. The method allowed us to measure Sr content in bone quantitatively down to 0.5 wt%.

Synchrotron radiation-induced micro-X-ray fluorescence (SR-μXRF) analysis

Distribution of the element Sr in bone at the level of bone packets was characterized using an elemental mapping method based on SR-μXRF analysis in confocal geometry.[22,23] The elemental mapping was done on bone surface areas identical to those examined previously by qBEI. The experiments were performed at the FLUO Beamline at ANKA, Karlsruhe, Germany.[22] To sufficiently excite the Sr K-lines, an excitation energy of 20 keV was chosen by means of a W/B_4C multilayer monochromator. The X-ray detector was an Oxford Pentafet 30 mm^2 Si(Li) detector with an 8 μm Be window.

The confocal setup was realized using two polycapillary half-lenses, one to focus the primary beam and the other to restrict the detector's field of view. The isotropic voxel size was $12 \times 12 \times 12\,\mu m^3$, and the counting time per voxel was 5 to 8 seconds. Mapping analyses have been performed on bone samples from one with 3 years of placebo treatment as reference and from two with 3 years of SrR treatment. The net intensities for Ca and Sr X-ray fluorescence spectra were determined by automatic peak fitting using the AXIL software from the QXAS package for peak deconvolution and subtraction of the radiation background. The resulting maps of net intensities were normalized to counts per second (cps) and 100 mA storage ring current and finally converted to 8-bit gray-scale images. The sensitivity of the method to detect traces of Sr in a bone matrix is about 100-fold higher than with the ERF-EDX method. Thus physiologic endogenous Sr content of bone (about 0.1 wt%) could be detected easily by this method.

Fourier transform infrared imaging (FTIRI) spectroscopic analysis

Trabeculae with evident formation of bone packets, determined based on qBEI images showing the presence of primary mineralization and no evidence of resorption (no evident resorption pits), were analyzed for collagen cross-links ratio spatial distribution using FTIRI. The ratio of two of the mineralizing type I collagen cross-links (pyr/deH-DHLNL) in bone-forming sites in trabecular bone was determined with a

spatial resolution of approximately 6.3 μm by FTIRI analysis using a Bruker Equinox 55 (Bruker Optics, Vienna, Austria) spectrometer interfaced with a mercury-cadmium-telluride (MCT) focal plane array detector (64 × 64 array) imaged onto the focal plane of an IR microscope (Bruker Hyperion 3000, Bruker Optics). For this purpose, approximately 4 μm thin sections were cut from the biopsy blocks and mounted between two barium fluoride windows. For the pyr:divalent collagen cross-link ratio, the amide I and II spectral regions were baseline corrected, and water vapor and PMMA were spectrally subtracted as published elsewhere.[24,25] The absorbance ratio at approximately 1660 and 1690 cm^{-1} was calculated. This ratio has been shown previously to correspond to the ratio of the pyr and divalent collagen cross-links.[24] Twelve biopsy samples from 6 patients treated for 3 years with placebo and 6 with SrR were analyzed this way.

Nanoindentation

Intrinsic mechanical properties of individual bone packets at the micron level were determined by nanoindentation experiments. The same sample blocks with the identical surface of sectioned bone area previously used for qBEI were investigated. Regions of interest (ROIs) containing bone packets of different ages as selected by previous qBEI (dark-gray levels = young and bright-gray levels = old tissue) were measured. The newly forming bone structural units (BSUs) chosen for nanoindentation consistently showed fluorescent bands when examined by fluorescence light microscopy. Several line scans with a step size of 20 μm were run through the trabecular features. In total, more than 100 indents per ROI about equally distributed over new and old bone areas were performed. A nanohardness tester (UBI-1, Hysitron, Inc., Minneapolis, MN, USA) equipped with a diamond tip of Berkovich type was employed. The indentation was done with a load of 5 mN, and the elastic modulus was derived from the unloading segment of the load-displacement curve based on the Oliver-Pharr method.[26] For more details of the applied method, see Gupta and colleagues.[27] For each biopsy sample, all the indents were collected and divided into two groups, indents coming from young and old bone packets, respectively. All 18 biopsy samples were analyzed in this way.

Statistical analysis

Statistical analysis was performed using Prism 4.0 (GraphPad Software, Inc., San Diego, CA, USA). Differences in BMDD parameters and collagen cross-link ratios were tested by *t* test or Mann-Whitney rank-sum tests if appropriate (Tables 1 and 2; see also Fig. 5). Linear regression analysis was performed for mean Sr at% (Sr/Sr + Ca) versus Sr serum level of patients (see Fig. 4), as well as for within-individual Sr at% (Sr/Sr + Ca) versus Ca content of young bone (see Fig. 3). Two-way ANOVA and paired *t* tests were used for the analysis of the nanoindentation data. For all analyses, $p < .05$ was considered significantly different.

Results

Transiliac biopsies from postmenopausal osteoporotic women treated for 3 years with placebo or with SrR were examined at the tissue level (level of bone packets) in multiple experimental approaches. The entire cancellous bone compartment of the transiliac biopsies was measured for BMDD using qBEI, and bone packets with different gray levels were selected for small-area ERF-EDX analysis and SR-μXRF mapping. Trabeculae with evident forming bone packets, determined based on qBEI images showing the presence of primary mineralization, were analyzed for collagen cross-links ratio spatial distribution using FTIRI. Young and old bone packets were examined by nanoindentation for mechanical properties.

1. BMDDs of paired biopsies ($n = 3$), before and after 3 years of SrR treatment, showed a distinct shift toward higher average atomic number after SrR treatment. On average ($n = 3$), Z_{mean} (ΔZ_{mean} + 2.0% and adΔZ_{mean} +4.7%) and Z_{peak} (ΔZ_{peak} +1.6% and adΔZ_{peak} +3.7%) were increased, the variations in the atomic numbers of the bone matrix Z_{width} (ΔZ_{width} −2.2% and adΔZ_{width} −19.5%) were reduced, and the amount of low mineralized bone Z_{low} (ΔZ_{low} −34.2%) was decreased after SrR treatment. The example of BMDDs from a pair of SrR treatment (SR0yrs and SR3yrs) shown in Fig. 1 illustrates this SrR treatment effect on BMDD. In contrast, no distinct changes can be seen after placebo treatment, as demonstrated in Fig. 1 by the placebo-treated pair of samples (PL0yrs and PL3yrs).
2. Group comparison of the BMDD parameters between placebo-treated ($n = 7$) and SrR-treated ($n = 7$) subjects resulted in significant differences (see Table 1). The group differences were for ΔZ_{mean} +1.5% and adΔZ_{mean} +3.6%, ($p < .05$), for ΔZ_{peak} +1.3% and adΔZ_{peak} +3.0% ($p < .05$), for ΔZ_{width} −3.1% and adΔZ_{width} −24.7% ($p < .01$), and for ΔZ_{low} −39.3% (NS). Comparison with previously published adult reference BMDD parameters revealed an increased Z_{mean} and Z_{peak} (for ΔZ_{mean} +1.4% and adΔZ_{mean} +3.3% and for ΔZ_{peak} +1.1% and adΔZ_{peak} +2.6%, respectively, both $p < .001$).
3. Group comparison of BMDD at baseline ($n = 4$) versus 36 months of placebo treatment ($n = 7$) revealed no significant differences in all four BMDD-parameters (see Table 2). Comparison of baseline BMDD with the adult reference BMDD also showed no differences with the exception of Ca_{width} (+15.8%, $p < .05$), which was increased. BMDD of after 3 years of placebo treatment ($n = 7$) also exhibited a significant increase only for Ca_{width} (+26.4%, $p < .001$) compared to the adult reference BMDD (see Table 2).
4. Selected-area ERF-EDX analysis (Fig. 2) revealed measurable local amounts of Sr predominantly in bone packets with relatively lower Ca content (Fig. 3) in a range from 3 to 6 at% [Sr/(Sr + Ca)].
5. This Sr atom fraction was independent of the variations in Ca content found in the young bone packets (correlation analysis revealed $p > .05$). One example of analysis is shown in Fig. 3.
6. Correlation analysis of the mean Sr at% [Sr/(Sr + Ca)] found in the young bone packets with serum levels of SrR showed a positive linear relationship ($r = 0.85$, $p = .018$; Fig. 4).
7. Highly sensitive elemental mapping combined with high spatial resolution using a SR-μXRF technique on bone surface areas identical to prior SEM/qBEI analysis confirmed in

Table 1. BMDD Parameters Derived From BMDD Calibrated in Units of *Z* (Average Atomic Number) of Normal Reference,[21] Baseline (PL-0) 3 Years, Placebo (PL-3) and 3 Year Treated Patients

	Ref ($n = 52$)	PL0yrs ($n = 4$)	PL3yrs ($n = 7$)	SrR3yrs ($n = 7$)
Z_{mean} (*Z*)	10.50	10.49	10.49	10.65*,****
	(10.42; 10.56)	(10.44; 10.50)	(10.24; 10.54)	(10.57; 10.75)
Z_{peak} (*Z*)	10.65	10.63	10.63	10.77*,****
	(10.60; 10.69)	(10.60; 10.65)	(10.39; 10.67)	(10.70; 10.88)
Z_{width} (*Z*)	6.68	6.78***	6.85****	6.64**
	(6.64; 6.71)	(6.75; 6.82)	(6.78; 6.85)	(6.59; 6.73)
Z_{low} (%)	4.52	5.14	6.16	3.74
	(3.87; 5.79)	(4.89; 5.50)	(4.52; 6.53)	(3.43; 6.61)

Data shown are median (25th percentile; 75th percentile).
*$p < .05$ and **$p < .01$ level of significance of differences between 3 years of placebo and 3 years of SrR.
***$p < .05$ and ****$p < .001$ level of significance of differences versus normal reference

both analyzed samples from SrR-treated patients that Sr is present predominantly in the lower-mineralized (young) bone packets, as demonstrated in Fig. 2. (#1, *a–c*). In adjacent older bone packets (see Fig. 2, #2, *a–c*), the Sr content was much lower (5- to 12-fold lower) so that it was not directly visible (gray level close to black) in the applied gray-scale setting.

8. Collagen cross-links ratio measurements of pyr/deH-DHLNL in the selected trabecular features using the FTIRI method did not detect significant alterations in cross-link patterns in the trabecular bone of the 6 biopsies from SrR-treated patients (mean pyr/deH-DHLNL $= 3.49 \pm 0.40$) compared with biopsies of the 6 placebo-treated patients (mean pyr/deH-DHLNL $= 3.40 \pm 0.22$) (Fig. 5).
9. Nanoindentation experiments on young compared with old bone packets revealed a significantly lower indentation modulus of young bone packets for the non-SrR-treated group (−20.5%, $p < .0001$, $n = 11$) as well as for the SrR-treated group (−24.3%, $p < .001$, $n = 7$). No selective influence of SrR treatment on these mechanical characteristics was observed in the dry conditions used (Fig. 6).

Table 2. BMDD Parameters Derived From BMDD Calibrated in Units of wt% Ca of Baseline, 3 Years Placebo-Treated Patients and Normal Reference[21]

	Ref ($n = 52$)	PL0yrs (n = 4)	PL3yrs ($n = 7$)
Ca_{mean} (wt% Ca)	22.23	22.15	22.14
	(21.84; 22.50)	(21.73; 22.25)	(20.93; 22.42)
Ca_{peak} (wt% Ca)	22.96	22.88	22.88
	(22.70; 23.14)	(22.53; 23.05)	(21.66; 23.0)
Ca_{width} (Δwt % Ca)	3.29	3.81*	4.16**
	(3.12; 3.47)	(3.639; 3.986)	(3.81; 4.16)
Ca_{low} (%)	4.52	5.14	6.16
	(3.87; 5.79)	(4.681; 5.825)	(4.52; 6.53)

Data shown are median (25th percentile; 75th percentile).
*$p < .05$ and **$p < .001$ level of significance of differences versus normal reference.

Discussion

Transiliac bone biopsies from postmenopausal osteoporotic women supplemented with calcium and vitamin D and treated for 3 years with or without SrR (placebo) were investigated by complementary methods at the bone material level to study the impact of strontium on bone material quality. A heterogeneous Sr uptake into individual BSUs (bone packets or osteons) was found with a distinct preference for bone packets formed during SrR treatment. SrR altered neither the collagen cross-links ratio nor the nanomechanical properties in the bones analyzed.

Effects on BMDD

Considering the BMDD measurements of patients before SrR treatment at baseline using qBEI, it is remarkable that their BMDD peak position (Ca_{peak}) was rather similar to that of a normal adult reference cohort,[21] except the heterogeneity of bone matrix mineralization within patients (Ca_{width}), which was slightly increased at baseline. This is somewhat different from earlier studies, where the increased Ca_{width} in the osteoporotic patients at baseline usually was accompanied by a shift toward lower mineralization densities.[28–30] The difference between the latter and the present observations is likely explained by the well-controlled pretreatment period with calcium/vitamin D (up to 6 months), whereas in the previous risedronate study[29] the calcium and vitamin D status was not adjusted to normal levels before study entry. Thus it seems that already 6 months of consequent calcium/vitamin D supplementation (in this SrR-treatment study 1000 mg Ca and 800 IU vitamin D daily) was sufficient to shift the BMDD toward normal levels. In consequence, after 3 years of placebo (plus calcium and vitamin D) treatment, the BMDD curve did not show any further changes compared with baseline. In our study, we observed in the SrR

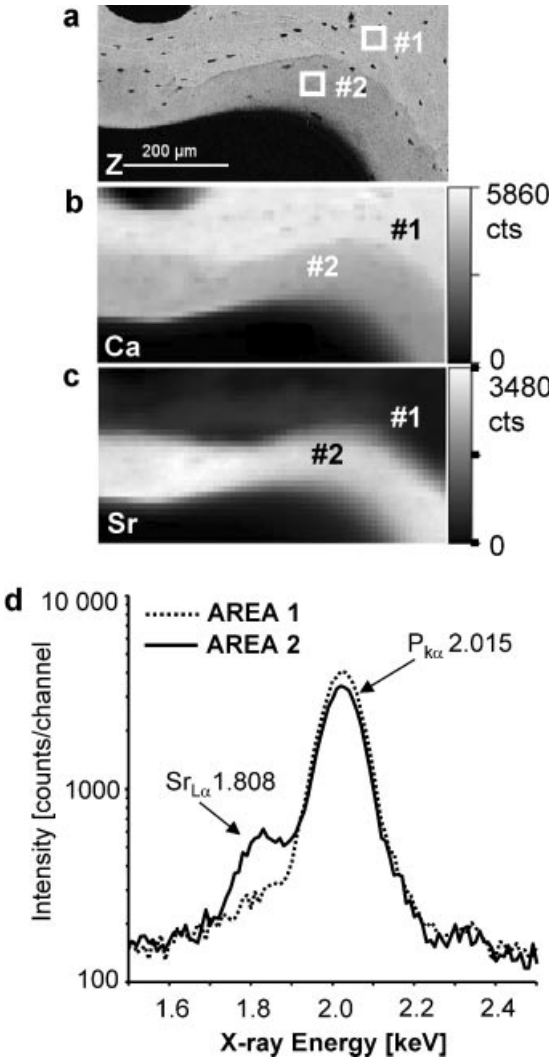

Fig. 2. Analysis of an identical trabecular bone feature from a patient treated with strontium ranelate by qBEI, ERF-EDX, and SR-µXRF. (*a*) qBEI displays a young bone packet (#2, less mineralized, darker gray levels) and adjacent older bone packet (#1, higher mineralized, brighter gray levels). (*b*) Elemental mapping of Ca using SR µ-XRF. (*c*) Elemental mapping of Sr using SR-µXRF; cts = normalized count rate of X-ray photons at Ca K-line and Sr K-line, respectively; packet #2 exhibited an average Sr intensity of 3066 cts and packet #1 an intensity of only 438 cts (intensity not visible because of gray level close to black/zero). (*d*) EDX spectra of area (within rectangular frames) #1 and #2 in (*a*) using ERF in the scanning electron microscope.

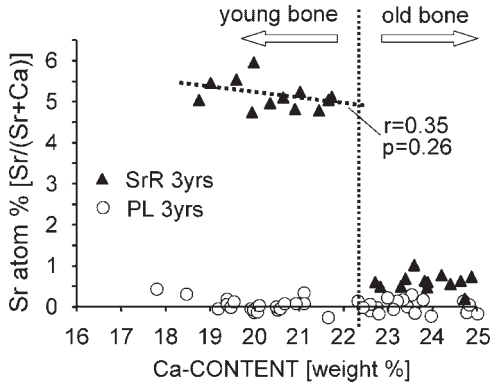

Fig. 3. Analysis of Sr and Ca content in single bone packets by ERF-EDX in one biopsy from a SrR-treated patient (SrR3yrs, *black triangle symbols*). Sr at% [Sr/(Sr + Ca)] values (*y* axis) are plotted versus Ca content (wt%) values (*x* axis): Young bone packets of relatively low Ca content have a measurable Sr content, whereas old bone packets exhibiting higher Ca content have only an Sr content that is at the limit of sensitivity of the ERF-EDX method (at 0.5 wt% Sr). Additional data points from placebo-treated patients (PL3yrs, *white circles symbols*) are indicated. All the data points are scattered around the zero level of Sr at% independently of Ca content. Thus the physiologic endogenous Sr content in non-SrR-treated bone is below the limit of sensitivity of the EFR-EDX method and therefore could not be quantified.

group a shift in the BMDD corresponding to a bone material with increased average atomic number (Z_{mean} and Z_{peak}) and a decrease in the range of variation in local atomic numbers (Z_{width}), as well as the amount of bone with low atomic numbers (Z_{low}), compared with baseline or placebo treatment. Usually, an increase in degree and homogeneity of mineralization can be interpreted as a reduction in bone turnover.[20]

However, the changes in the BMDD curves in SrR-treated patients have to be interpreted with caution. Independent of potential effects on bone resorption or formation, the uptake of Sr into the bone matrix generates a higher backscattered electron signal than calcium (effect of atomic number Sr, Z = 38, versus Ca, *Z* = 20) and has to be taken into account. The fact that Sr is preferentially incorporated into the bone packets formed during the 3 years of SrR treatment favors this type of change in BMDD together with the amount (percentage) of these new bone packets, as well as their age distribution, which influences the extent of the atomic number effect on the individual BMDD. It has to be mentioned that similar to the results of the qBEI method, the atomic number effect of Sr can lead to an overestimation of mineral content in microradiographic[15] as well as dual-energy X-ray absorptiometry (DXA)[31] measurements because of the higher absorbance for Sr by X-rays compared with Ca. Thus observed increases in BMD[2,3] also have to be interpreted with caution because they represent the sum of changes in bone volume, degree of mineralization,[30] and additionally, amount of incorporated Sr.[31,34]

Moreover, the qBEI analysis revealed that neither rickets nor a decrease in mineralization was induced by SrR treatment in any of the samples we have investigated. This confirms results from the histomorphometric evaluation carried out on a much higher number of samples (>30), which showed the absence of a deleterious effect of SrR on the primary mineralization of bone.[6] This can be related to the calcium/vitamin D supplementation before and during the whole study period, together with the relatively low SrR dose used. Indeed, the importance of an adequate Ca intake in SrR treatment has to be emphasized because high doses of strontium induced mineralization defects in animals with a Ca-depleted diet.[35–37] In a rat study of SrR treatment, it has been demonstrated recently that insufficient Ca intake can lead to an absorption of up to 6 times more Sr than under a normal Ca diet.[7]

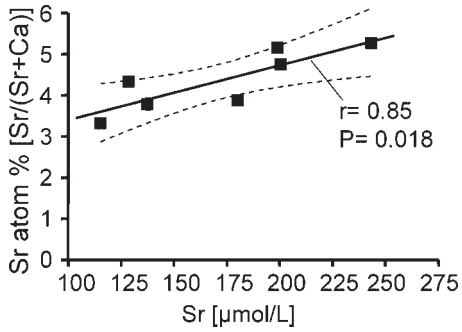

Fig. 4. Relationship between average Sr at% [Sr/(Sr + Ca)] in bone packets ($n \cong 10$) newly formed during SrR treatment and the corresponding Sr serum level found in the patients ($n = 7$) after a 3-year treatment. Error bars of SEM are smaller than symbol size.

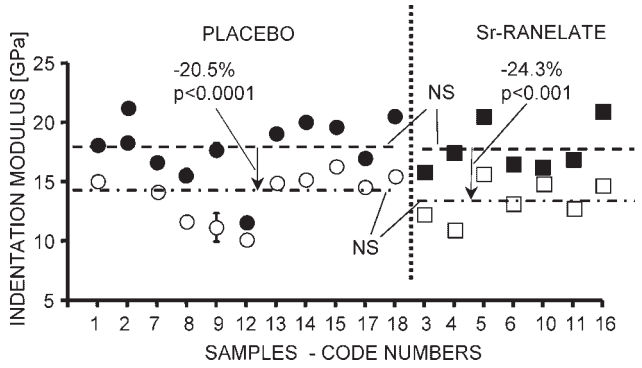

Fig. 6. Comparison of nanoindentation modulus on bone packets from PL0yrs ($n = 3$), SrR0yrs ($n = 1$), PL3yrs ($n = 7$), and SrR3yrs ($n = 7$) patients (in total, $n = 18$). Number of indents within each bone packet category (young versus old) was around 50 (total of 100 indents per sample). Open symbols = young bone packets; full symbols = old bone packets, as judged from gray levels of qBEI. Error bars of SEM are mostly smaller than symbol size. Dashed line indicates mean level of old bone; dashed-pointed line indicates mean level of young bone.

Distribution of Sr in bone tissue

Electron-induced X-ray fluorescence analysis in combination with backscattered electron imaging in the scanning electron microscope of individual bone packets revealed an Sr uptake of up to 6% atom fraction [Sr/(Sr + Ca)], which would correspond to the replacement of 1 Ca ion by 1 Sr ion out of 16 Ca atoms in the mineral crystal lattice or 0.6 Sr ions per 10 Ca ions. This is about half the maximum reported in the monkey treatment model with 1.2 Sr ions per 10 Ca ions, which can be accounted for by the higher dose levels used in monkeys.[15] The major Sr uptake occurred in the newly formed bone packets (formed during SrR treatment), consistent with previously described outcomes in human patients[17,32] and in animal studies.[14,15] This preferential uptake in relatively young bone packets also was confirmed by the applied highly sensitive and spatially resolved elemental mapping method using SR-µXRF. Moreover, it has to be emphasized that the atomic fraction of Sr remains constant and is independent of the actual Ca content of the bone packets formed during SrR treatment within an individual patient. However, the Sr fraction value is positively correlated with the Sr serum level found in individual patients. These results are in agreement with previous studies of Sr uptake in animal models[16] and a recent human study.[17] All together, the data suggest that when the BSU is formed and the osteoid starts to be mineralized in the presence of a certain Sr to Ca fraction in the interstitial fluid of bone tissue, Sr is incorporated with a certain fraction into the crystal from the beginning of crystal growth but is not a result of long-lasting diffusion exchange processes after crystal growth has occurred. As a consequence, the Sr fraction remains constant during the entire growth period of the mineral crystal in the phase of primary and secondary mineralization. This also may explain why bone packets formed under SrR treatment, having different age/mineral content, exhibited a similar Sr fraction within one individual, whereas in older bone packets that have passed a long period of secondary mineralization

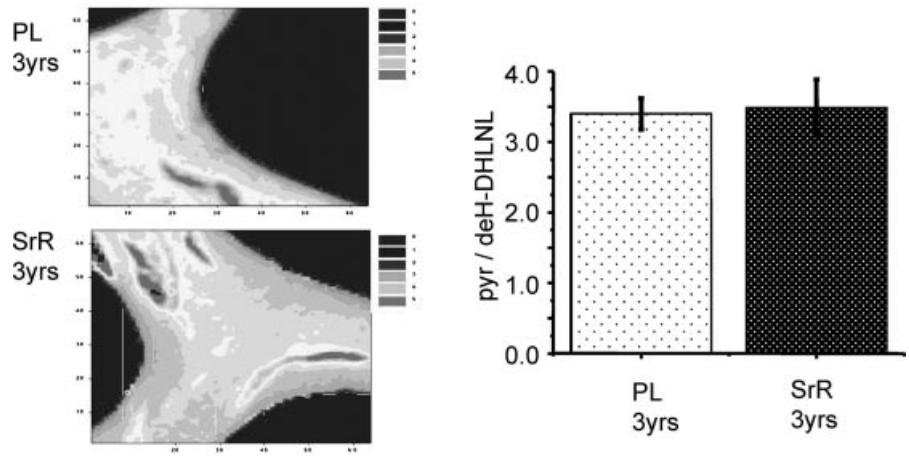

Fig. 5. Collagen cross-links ratio (pyr/deH-DHLNL) mapping (images) and quantification (bar diagram) of trabecular bone features using FTIRI. PL3yrs = 3 years placebo treatment of patients ($n = 6$), SrR3yrs = 3yrs SrR treatment of patients ($n = 6$). Trabeculae analyzed were selected based on previously acquired qBEI images. The surfaces were devoid of resorption pits, and at least one surface exhibited primary mineralization.

without being exposed to Sr in the serum had relatively small amounts of Sr. It is likely that in older bone packets crystal growth has been slowed down, and only a few atoms are added to the surface of preexisting crystals. In addition, potential ion exchanges by diffusion are assumed to be slow. However, to clarify the nature of Sr incorporation in the young bone packets, spatially resolved techniques such as scanning X-ray diffraction (XRD) by synchrotron radiation experiments were performed and are reported in Li and colleagues.[33] The latter and present studies taken together show that Sr is taken up during bone formation and that the amount being incorporated into the mineral crystal depends on the serum level of Sr during treatment. In our patients group, a serum Sr level of up to 250 μmol/L was found, which generated an average Sr content in bone packets formed during SrR treatment of up to 5 at%, as measured focally by ERF-EDX. Consistently, scanning synchrotron X-ray diffraction by Li and colleagues[33] revealed changes in the crystal lattice constant corresponding to a 5 at% incorporation of Sr. In consequence, for the whole Sr content in bone accumulated during SrR treatment, two mechanism have to be taken into account: First, as stated earlier, every bone packet formed during SrR treatment within an individual will have the same characteristic Sr to Ca fraction, and the absolute Sr value is increasing according to the increase in the Ca content with duration of secondary mineralization of the bone packet. Second, since bone remodeling is an ongoing process, it has to be assumed that, theoretically, at some time point (depending on the bone turnover rate) all "old" bone packets (preexisting SrR treatment) will have been removed and replaced by "new" bone packets (formed during SrR treatment) with a characteristic Sr to Ca fraction within their mineral crystals. This would represent the maximal level of Sr that can be achieved in bone. Hence the resulting Sr content depends strongly on local bone remodeling activity and duration of treatment at specific serum level of Sr. Indeed, the Sr content has been found to be variable at different skeletal sites depending on bone turnover[16] and to be increasing in transiliac bone with duration of SrR treatment. A progressive increase in global Sr content (measured chemically) from 1 to 3 years with no further increase from 3 to 5 years was reported.[17] In contradiction, measurements on ultra–distal radius using a special noninvasive DXA method revealed, however, a continuous increase in Sr for up to 8 years of treatment, which is very controversial and remains an open matter.[38–40]

Sr uptake and collagen cross-linking

Using a FTIRI technique, the average collagen cross-link ratio of the trabecular bone features formed under SrR and placebo treatment was studied. No changes compared with placebo treatment could be detected. This is in contrast to other treatments, where significant changes were observed,[41,42] and indicates that SrR does not seem to interfere with collagen cross-link formation.

Sr incorporation and bone material elastic modulus

Nanoindentation analysis was performed to determine the mechanical properties of the collagen/mineral bone nanocomposite material after SrR treatment. There was a lower indentation modulus for young compared with old bone packets that was significant, as classified by their lower or higher mineral content, respectively. No differences were observed between the placebo and SrR groups, meaning that the newly deposited bone matrix, which is added to and/or is exchanged with the old bone matrix in patients treated with SrR, is of the same quality, and hence SrR does not compromise the nanomechanical properties of bone material.

Furthermore, it has to be emphasized that the entire study is based on undecalcified PMMA-embedded bone tissue. This preparation method includes fixation in 70% ethanol followed by dehydration using 100% ethanol. Thus Ca and Sr of the soluble phase and the fast exchangeable pool in the interstitial fluid and intrinsic surfaces in the bone tissue containing about 0.65% of the total skeletal Ca[11] might be lost, and predominantly, the substituted Sr is present in the sample blocks for measurement. Moreover, it is known that the bone material exhibits different mechanical behaviors, depending on the hydration state of the sample.[43] While in wet condition, altered nanomechanical parameters were observed in SrR-treated rat bone compared with nontreated bone,[8,44] there was no such difference between the groups in dry bone samples,[44] which is consistent with our results.

Conclusion

In conclusion, strontium ranelate (SrR) treatment does not alter determinants of bone material quality such as degree of mineralization, collagen cross-linking, and indentation modulus compared with the placebo-treated group. Only the bone tissue formed during SrR treatment (2 g/d) shows Sr incorporation up to 6 at% [Sr/(Sr + Ca)] after 3 years of treatment. Taken together, these data provide evidence that the bone quality determinants at the tissue level, including degree of mineralization, collagen cross-linking, and intrinsic bone mechanical characteristics, are preserved after a 3-year SrR treatment in postmenopausal osteoporotic women.

Disclosures

All the authors state that they have no conflicts of interest.

Acknowledgments

We are most grateful to Dr Isabelle Dupin-Roger of the Institut de Recherches Internationales SERVIER (IRIS), Courbevoie, France, for many useful discussions and a critical reading of this paper. Further, we thank G Dinst, S Thon, Ph Messmer, and D Gabriel for careful sample preparation and qBEI and EDX measurements. This study was supported by research grants from Servier, the Research Funds of the Austrian Workers Compensation Board (AUVA), and the Viennese Sickness Insurance Funds (WGKK).

References

1. Meunier PJ, Roux C, Seeman E, et al. The effects of strontium ranelate on the risk of vertebral fracture in women with postmenopausal osteoporosis. N Engl J Med. 2004;350:459–468.

2. Reginster JY, Seeman E, De Vernejoul MC, et al. Strontium ranelate reduces the risk of nonvertebral fractures in postmenopausal women with osteoporosis: treatment of peripheral osteoporosis (TROPOS) study. J Clin Endocrinol Metab. 2005;90:2816–2822.
3. Reginster JY, Felsenberg D, Boonen S, et al. Effects of long-term strontium ranelate treatment on the risk of nonvertebral and vertebral fractures in postmenopausal osteoporosis. Arthritis Rheum. 2008;58:1687–1695.
4. Seeman E, Devogelaer JP, Lorenc R, et al. Strontium ranelate reduces the risk of vertebral fractures in patients with osteopenia. J Bone Miner Res. 2008;23:433–438.
5. Marie PJ. Strontium ranelate: a pharmacological approach for optimizing bone formation and resorption. Bone. 2006;38:S10–S14.
6. Arlot ME, Jiang Y, Genant HK, et al. Histomorphometric and MCT analysis of bone biopsies from postmenopausal osteoporotic women treated with strontium ranelate. J Bone Miner Res. 2008;23:215–222.
7. Fuchs RK, Allen MR, Condon KW, et al. Strontium ranelate does not stimulate bone formation in ovariectomized rats. Osteoporosis Int. 2008;19:1331–1341.
8. Bain SD, Jerome C, Shen V, Dupin-Roger I, Ammann P. Strontium ranelate improves bone strength in ovariectomized rat by positively influencing bone resistance determinants. Osteoporos Int. 2008; preprint 0:1–12
9. Brennan TC, Rybchyn MS, Green W, Atwa S, Conigrave AD, Mason RS. Osteoblast play key roles in the mechanisms of action of strontium ranelate. British Journal of Pharmacology. 2009; (in press).
10. Hurtel-Lemaire AS, Mentaverri R, Caudrillier A, et al. The calcium-sensing receptor is involved in strontium ranelate-induced osteoclast apoptosis. J Biological Chemistry. 2009;284:575–584.
11. Skoryna SC. Effects of oral supplementation with stable strontium. CMA Journal. 1981;125:703–712.
12. Ammann P, Shen V, Robin B, Mauras Y, Bonjour JP, Rizzoli R. Strontium ranelate improves bone resistance by increasing bone mass and improving architecture in intact female rats. J Bone Miner Res. 2004;19:2012–2020.
13. Grynpas MD, Hamilton E, Cheung R, et al. Strontium increases vertebral bone volume in rats at a low dose that does not induce detectable mineralization defects. Bone. 1996;18:253–259.
14. Boivin G, Deloffre P, Perrat B, et al. Strontium distribution and interactions with bone mineral in monkey iliac bone after strontium salt (S 12911) administration. J Bone Miner Res. 1996;11:1302–1311.
15. Farlay D, Boivin G, Panczer F, Lalande A, Meunier JP. Long-term strontium ranelate administration in monkeys preserves characteristics of bone mineral crystals and degree of mineralization of bone. J Bone Miner Res. 2005;20:1569–1578.
16. Dahl SG, Allain P, Marie PJ, et al. Incorporation and distribution of strontium in bone. Bone. 2001;28:446–453.
17. Boivin G, Farlay D, Khebbab MT, Jaurand X, Delmas PD, Meunier PJ. In osteoporotic women treated with strontium ranelate, strontium is located in bone formed during treatment with a maintained degree of mineralization. Osteoporos Int. 2009 Jul 14.
18. Roschger P, Plenk H Jr, Klaushofer K, Eschberger J. A new scanning electron microscopy approach to the quantification of bone mineral distribution: backscattered electron image grey-levels correlated to calcium K alpha-line intensities. Scanning Microsc. 1995;9:75–86; discussion 86-8.
19. Roschger P, Fratzl P, Eschberger J, Klaushofer K. Validation of quantitative backscattered electron imaging for the measurement of mineral density distribution in human bone biopsies. Bone. 1998;23:319–326.
20. Roschger P, Paschalis EP, Fratzl P, Klaushofer K. Bone mineralization density distribution in health and disease. Bone. 2008;42: 456–466.
21. Roschger P, Gupta HS, Berzlanovich A, et al. Constant mineralization density distribution in cancellous human bone. Bone. 2003;32:316–323.
22. Zoeger N, Streli C, Wobrauschek Jokubonis C, et al. Determination of the elemental distribution in human joint bones by SR micro XRF. X-Ray Spectrometry. 2008;37:3–11.
23. Zoeger N, Roschger P, Hofstaetter JG, et al. Lead accumulation in tidemark of articular cartilage. Osteoarthritis and Cartilage. 2006;14:906–913.
24. Paschalis EP, Verdelis K, Doty SB, Boskey AL, Mendelsohn R, Yamauchi M. Spectroscopic characterization of collagen cross-links in bone. J Bone Miner Res. 2001;16:1821–1828.
25. Paschalis EP, Recker R, DiCarlo E, Doty SB, Atti E, Boskey AL. Distribution of collagen cross-links in normal human trabecular bone. J Bone Miner Res. 2003;18:1942–1946.
26. Oliver W, Pharr G. An improved technique for determining hardness and elastic modulus using load and displacement sensing indentation experiments. J Mater Res. 1992;4:1564–1583.
27. Gupta SH, Schratter S, Tesch W, et al. Two different correlations between nanoindentation modulus and mineral content in the bone-cartilage interface. Journal of Structural Biology. 2005;149: 138–148.
28. Roschger P, Rinnerthaler S, Yates J, Rodan GA, Fratzl P, Klaushofer K. Alendronate increases degree and uniformity of mineralization in cancellous bone and decreases the porosity in cortical bone of osteoporotic women. Bone. 2001;29:185–189.
29. Zoehrer R, Roschger P, Fratzl P, et al. Effects of 3- and 5-year treatment with Risedronate on the bone mineral density distribution of cancellous bone in human iliac crest biopsies. J Bone Miner Res. 2006;21:1106–1112.
30. Fratzl P, Roschger P, Fratzl-Zelman N, Paschalis EP, Phipps R, Klaushofer K. Evidence that treatment with Risedronate in women with postmenopausal osteoporosis effects bone mineralization and bone volume. Calcif Tissue Int. 2007;81:73–80.
31. Blake GM, Fogelman I. The correction of BMD measurements for bone strontium content. J Clin Densitom. 2007;10:259–265.
32. Boivin G, Meunier PJ. The mineralization of bone tissue: a forgotten dimension in osteoporosis research. Osteoporosis Int. 2003;14:S19–S24 (Review).
33. Li C, Paris O, Siegel S, et al. Strontium is incorporated into mineral crystals only in newly formed bone during strontium ranelate treatment [published online ahead of print October 26, 2009] J Bone Miner Res. doi:10.1359/jbmr.091038.
34. Kendler DL, Adachi JD, Josse RG, Slosman DO. Monitoring strontium ranelate therapy in patients with osteoporosis. Osteoporosis Int. DOI 10.1007/s00198-009-0886-1.
35. Sobel AE, Cohen J, Kramer B. The nature of the injury to the calcifying mechanism in rickets due to strontium. Biochem J. 1935;29:2640–2646.
36. Storey E. Intermittent bone changes and multiple cartilage defects in chronic strontium rickets in rats. J Bone Joint Surg. 1962;44B:194–208.
37. Omdahl JL, DeLuca HF. Strontium induced rickets: metabolic basis. Science. 1971;174:949–951.
38. Bärenholdt O, Kolthoff N, Nielsen SP. Effect of long-term treatment with strontium ranelate on bone strontium content. Bone. 2009;45:200–206.
39. Belissa-Chatelain P, Dupin-Roger I, Cournarie F, Tsouderos Y. Re: "Effect of long-term treatment with strontium ranelate on bone strontium content" by Bärenholdt et al. (Bone, 2009). Bone. 2009 Jul 17. [Epub ahead of print].
40. Bärenholdt O, Kolthoff N, Nielsen SP. Reply to Letter Re: "Effect of long term treatment with strontium ranelate on bone strontium

content'' by Bärenholdt et al. (Bone, 2009). Bone. 2009 Jul 17. [Epub ahead of print].

41. Paschalis EP, Glass EV, Donley DW, Eriksen EF. Bone mineral and collagen quality in iliac crest biopsies of patients given teriparatide: new results from the fracture prevention 26 trial. J Clin Endocrinol Metab. 2005;90:4644–4649.
42. Durchschlag E, Paschalis EP, Zoehrer R, et al. Bone material properties in trabecular bone from human iliac crest biopsies after 3- and 5-year treatment with risedronate. J Bone Miner Res. 2006;21:1581–1590.
43. Zysset PK, Guo XE, Hoffler CE, Moore KE, Goldstein SA. Elastic modulus and hardness of cortical and trabecular bone lamellae measured by nanoindentation in the human femur. J Biomech. 1999;32:1005–1012.
44. Ammann P, Badoud I, Barraud S, Dayer R, Rizzoli R. Strontium ranelate treatment improves trabecular and cortical intrinsic bone tissue quality, a determinant of bone strength. J Bone Miner Res. 2007;22:1419–1425. Erratum in: J Bone Miner Res. 2007 Nov;22(11): 1828.